= 145 Hz mP^{-1} when T_1^{-1}/η = 12 Hz mP^{-1} for PC) could be due to a distortion of the solvation shell by the bulky tetraphenylborate anion, in proximity of the complexed sodium, in a low dielectric solvent (ϵ = 12.9).

The enthalpy-entropy compensation effect that we have observed and discussed in the case of (DB18C6, Na^+) is also operative for (18C6, Na^+). The same effect is well documented for thermodynamic data.[30]

For the bimolecular mechanism, ΔG^* varies in the order PC < AN < PY. This trend suggests that the major contribution to the exchange barrier is the desolvation of the incoming cation.

Despite the differences in the ridigity of the ligand, in the basicity of the ether oxygens, and in the structure of the complexes in solution, there is a remarkable similarity between the activation parameters for the dissociation of (DB18C6, Na^+)[10] and (18C6, Na^+) in acetonitrile. Direct comparison is possible since the unimolecular exchange rates were obtained under similar experimental conditions. ΔG^*_{300K} is 53 kJ·mol^{-1} for both systems.

The lower enthalpy of activation for (18C6, Na^+) is compensated for by a lower entropy of activation. The more flexible 18C6 gives rise to a lower activation enthalpy. The fact that the activation parameters for both systems are comparable is another indication of the role of the solvent in the barrier of dissociation.

Conclusion

In the four nonaqueous solvents of this study, the sodium cation exchanges between solvated and 1:1 complexed sites when it is in the presence of 18-crown-6. The exchange follows two mechanisms which are competitive. The determination of the pseudo-first-order rate constants for the exchange for various concentrations and temperatures allows the separation of both contributions to the exchange. In favorable cases, such as propylene carbonate, it is possible to determine the activation enthalpy and entropy for both processes. The mechanism is almost exclusively unimolecular in acetone. In pyridine, acetonitrile, and propylene carbonate, both mechanisms are in competition. Our results show that the unimolecular decomplexation is the product of several factors, the least of which is not the role of the solvent. In general, there is a compensation effect for the enthalpy and the entropy of activation. In particular, this effect is at the origin of the identical free energy of activation for (18C6, Na^+) and (DB18C6, Na^+) in acetonitrile.

Acknowledgment. The Natural Sciences and Engineering Research Council of Canada (NSERCC) is acknowledged for financial support.

Registry No. Na, 7440-23-5; (18-crown-6, Na^+), 31270-12-9.

Is Bound CO Linear or Bent in Heme Proteins? Evidence from Resonance Raman and Infrared Spectroscopic Data

Xiao-Yuan Li and Thomas G. Spiro*

Contribution from the Department of Chemistry, Princeton University, Princeton, New Jersey 08544. *Received July 22, 1987*

Abstract: The vibrational data on heme-CO complexes are analyzed with a view toward elucidating the structural evidence for distorted FeCO units in heme proteins. The effects of FeCO distortion on the vibrational frequencies are attributable to back-bonding changes, as evidenced by the correlation of ν_{FeC} with ν_{CO}. Steric restraint of perpendicular binding increases Fe → CO back-donation slightly. This is opposite to the direction expected if the FeCO unit is bent but is consistent with the expected effect of two other distortion coordinates, FeCO tilting and porphyrin buckling. Larger effects on back-bonding are attributable to polar interactions of distal residues with the bound CO, especially H bonding. Substantial FeCO bending is inconsistent with the relatively small frequency separation between ν_{FeC} and δ_{FeCO} observed in all adducts so far examined; this separation is calculated to increase strongly with the bending angle due to mixing of the modes. For a given displacement of the O atom from the heme normal, the energy required for the three distortion coordinates is calculated to increase in the order tilting < buckling < bending. The energy is minimized, as are the individual angular displacements, if all three contribute to the actual molecular distortion, and the small net change may result from the opposing effects of bending and of tilting and buckling in ν_{FeC}. This concerted model of FeCO distortion is not inconsistent with the available X-ray crystal structure data. It is inconsistent with EXAFS analysis of MbCO at 4 K, which has yielded a small value, 127 ± 4°, for the FeCO angle from the attenuation of second-shell scattering relative to a protein-free model. This attenuation might be due instead to other changes in second-shell scattering, e.g. due to porphyrin buckling.

Introduction

X-ray and neutron scattering crystal structures are available for the carbon monoxide adducts of several heme proteins.[1] An interesting observation is that nonbonded contacts in the heme pocket frequently prevent the bound CO from adopting its expected configuration, namely a linear FeCO unit normal to the heme plane. This structure, established crystallographically for several protein-free CO adducts of iron(II) porphyrins,[2] is the one expected from considerations of maximum orbital overlap in the well-established π back-donation bonding model for transition-metal carbonyls. Deviations from this geometry are expected to cost energy, and it has been suggested by Collman and co-workers[3] that the steric hindrance seen in heme proteins may play a functional role in lowering the CO affinity, thereby raising the threshold for CO poisoning. Whether the CO affinity is actually

(1) (a) Kuriyan, J.; Wiltz, S.; Karplus, M.; Petsko, G. *J. Mol. Biol.* **1986**, *192*, 133-154. (b) Hanson, J. C.; Schoenborn, B. P. *J. Mol. Biol.* **1981**, *153*, 117. (c) Baldwin, J. M.; Chothia, C. *J. Mol. Biol.* **1979**, *129*, 175. (d) Baldwin, J. M. *J. Mol. Biol.* **1980**, *136*, 103. (e) Steigeman, W.; Weber, E. *J. Mol. Biol.* **1979**, *127*, 309. (f) Tucker, P. W.; Philipps, S. E. V.; Perutz, M. F.; Houtchens, R. A.; Caughey, W. S. *Proc. Natl. Acad. Sci. U.S.A.* **1978**, *75*, 1076. (g) Heidner, E. J.; Ladner, R. C.; Perutz, M. F. *J. Mol. Biol.* **1976**, *104*, 707. (h) Norvell, J. C.; Nunes, A. C.; Schoenborn, B. P. *Science (Washington, D.C.)* **1975**, *190*, 568. (i) Padlan, E. A.; Love, W. E. *J. Biol. Chem.* **1974**, *249*, 4067. (j) Huber, R.; Epp, O.; Formanek, H. *J. Mol. Biol.* **1970**, *52*, 349.

(2) (a) Peng, S. M.; Ibers, J. A. *J. Am. Chem. Soc.* **1976**, *98*, 8032. (b) Scheidt, W. R.; Haller, K. J.; Fons, M.; Fashiko, T.; Reed, C. A. *Biochemistry* **1981**, *20*, 3653. (c) Caron, C.; Mitschler, A.; Riviere, G.; Ricard, L.; Schappacher, M.; Weiss, R. *J. Am. Chem. Soc.* **1979**, *101*, 7401.

(3) (a) Collman, J. P.; Brauman, J. I.; Halbert, T. R.; Suslick, K. S. *Proc. Natl. Acad. Sci. U.S.A.* **1976**, *73*, 3333. (b) Collman, J. P.; Brauman, J. I.; Everson, B. L.; Sessler, J. L.; Morris, R. M.; Gibson, Q. H. *J. Am. Chem. Soc.* **1983**, *105*, 3052.

0002-7863/88/1510-6024$01.50/0

Table I. Structures of Heme–CO Adducts[a]

molecule	resolution, Å	FeCO geometry	ref
sperm whale Mb	1.5	bent θ = 140 and 120°	1a
sperm whale Mb (neutron)	1.8	tilted ϕ = 24°	1b
human Hb	2.7	tilted ϕ = 13°	1c, 1d
erythrocruorin	1.4	tilted ϕ = 19°	1e
Hb Zurich [His E_7 (63) → Arg]	2.8	tilted	1f
Hb Sydney [Val E11 (67) → Ala]			
horse Hb	2.8	tilted	1g
sperm whale Mb[b] (neutron)	1.8	bent θ = 135°	1h
Glycerqa dibranchiata Hb	2.5	tilted ϕ = 45°	1i
sperm whale Mb (EXAFS)		bent θ = 127 ± 4°	6
$PyFe^{II}TPP$		linear θ = 179 ± 2° ϕ = 2.5 ± 0.8°	2a
$(THF)Fe^{II}$(deuteroporphyrin)		linear θ = 178.3° ϕ = 2.6°	2b
$(C_2H_5S)Fe^{II}$(tetraphenylporphine)		linear	2c

[a] X-ray crystallographic, unless otherwise noted. [b] Same data set as ref 1b.

lowered significantly in heme proteins has been questioned by Traylor,[4] and Mims et al.,[5] on the basis of affinity comparisons with model systems, although steric hindrance is clearly capable of lowering CO affinity.[3b]

Whatever the energetic consequences, it does appear certain that, in several well-characterized protein crystal structures (see Table I), the O atom of the bound CO deviates significantly from the normal to the heme plane. The deviation has in some cases been modeled as a bend of the FeCO unit at the C atom and in others as a tilt at the Fe atom. The Fe–C–O angle is difficult to determine accurately, especially as there is a tendency to disorder in the CO positions; this disorder has been analyzed in the recent high-resolution (1.5 Å) crystal structure of MbCO (Mb = myoglobin) by Kuriyan et al.[1a] EXAFS (extended X-ray absorption fine structure) data on the CO adduct of myoglobin have been interpreted in terms of a bent structure.[6] In this case the evidence comes from the amplitude of second-shell scattering, which is elevated for linear FeCO by the self-focusing effect of the intervening C atom; this amplitude was found to be significantly lower in MbCO than for a protein-free model, and a FeCO angle of 127 ± 4° was calculated.

Vibrational spectroscopy is capable of providing detailed structural information about bound CO. The CO stretching frequency ~1950 cm^{-1} is in a blank region of the infrared spectrum, and it has been possible to record ν_{CO} in proteins as well as model compounds.[7] In resonance Raman (RR) spectra, one can readily detect the Fe–C stretching mode, and frequently the Fe–C–O bending mode as well, enhanced via coupling with the strong heme Soret electronic transition.[8] The CO stretching mode, although enhanced only weakly, can sometimes be seen in RR spectra. There is now a substantial body of data on numerous heme CO species (see Table II). A general inverse correlation between ν_{CO} and ν_{FeC} can be observed,[8,9] as expected from the

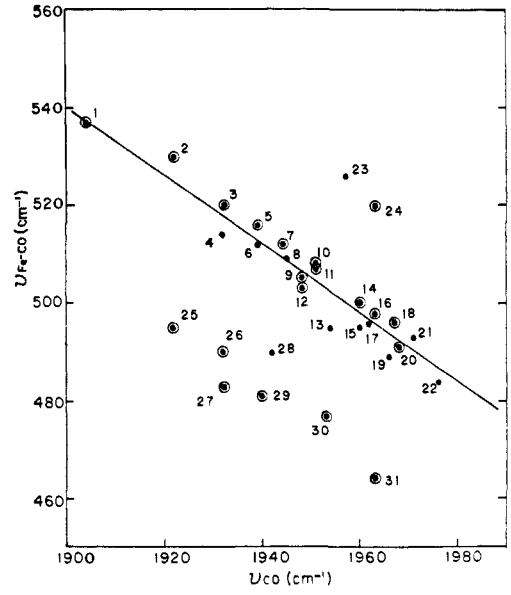

Figure 1. Plot of observed ν_{FeC} vs ν_{CO} adducts of heme proteins (circles) and analogue complexes (dots). The numbers correspond to the entries in Table II.

back-bonding model of CO binding to Fe^{II}. Specific effects have also been noted for H bonding to the bound CO in the heme pocket[10,11] and for differences in the trans axial ligand.[8-11] There is, however, uncertainty about how to deal with the likely effects on the vibrational spectrum of protein-induced distortions in the FeCO unit itself. Yu and co-workers, who have been responsible for the RR assignments and for much of the available data, have considered this matter in some detail.[12] They proposed an approximate equation with which the FeCO angle can be calculated from isotope shifts of the ν_{CO} and ν_{FeC} modes. These calculations showed the FeCO angle to be within experimental error of 180° for most cases, and it was suggested that protein-induced distortions result mainly in tilting rather than bending of the FeCO unit. Unfortunately, the equation proposed by Yu et al.[12] can be shown on theoretical grounds to be unreliable since terms neglected in its derivation are larger than those retained. This point is discussed in the Appendix, where it is shown that the FeCO angle cannot be calculated reliably from the vibrational frequencies and isotope shifts.

We have examined the sensitivity of the vibrational spectrum to the FeCO geometry with model normal coordinate calculations, using the available data as a guide. FeCO bending and tilting are both considered, and a third plausible distortion coordinate, porphyrin buckling, is introduced. Our conclusion is that the vibrational data are *inconsistent* with a large degree of FeCO bending, whose kinematic and electronic consequences are expected to be profound. Neither FeCO tilting nor porphyrin buckling are inconsistent with the data, since kinematic effects are inconsequential and electronic effects are likely to be in the right direction. Their influence may well be masked, however, by other electronic effects, particularly those associated with the trans ligand and with polar interactions in the CO binding region. The energetics of off-axis binding are analyzed in terms of the force constants and

(4) (a) Traylor, T. G.; Campbell, D.; Tsuchiya, S.; Stynes, D. V. *J. Am. Chem. Soc.* **1980**, *102*, 5939. (b) Traylor, T. G. *Acc. Chem. Res.* **1981**, *14*, 102.

(5) Mims, M. P.; Porras, A. G.; Olson, J. S.; Noble, R. W.; Peterson, J. A. *J. Biol. Chem.* **1983**, *258*, 14219.

(6) Powers, L.; Sessler, J. L.; Woolery, G. L.; Chance, B. *Biochemistry* **1984**, *23*, 5519.

(7) (a) Barlow, C. H.; Ohlsson, P.-I.; Paul, K.-G. *Biochemistry* **1976**, *15*, 2225. (b) Yoshikawa, S.; Choc, M. G.; O'Toole, M. C.; Caughey, W. S. *J. Biol. Chem.* **1977**, *252*, 5498. (c) Makinen, M. W.; Houtchens, R. A.; Caughey, W. S. *Proc. Natl. Acad. Sci. U.S.A.* **1979**, *76*, 6042. (d) Shimada, H.; Caughey, W. S. *J. Biol. Chem.* **1982**, *257*, 11893. (e) Paul, K.-G.; Smith, M. L.; Ohlsson, P.-I. *Inorg. Chim. Acta* **1983**, *79*, 169. (f) Smith, M. L.; Ohlsson, P.-I.; Paul, K.-G. *FEBS Lett.* **1983**, *163*, 303. (g) Brown, W. E., III; Sutcliffe, J. W.; Pulsinelli, P. D. *Biochemistry* **1983**, *22*, 2914.

(8) Kerr, E. A.; Yu, N. T. In *Biological Applications of Raman Spectroscopy*; Spiro, T. G., Ed.; Wiley-Interscience: New York, 1988; Vol. III, Chapter 2.

(9) (a) Tsubaki, M.; Ichikawa, Y. *Biochim. Biophys. Acta* **1985**, *827*, 268. (b) Paul, J.; Smith, M. L.; Paul, K.-G. *Biochim. Biophys. Acta* **1985**, *832*, 257. (c) Uno, T.; Nishimura, Y.; Tsuboi, M.; Makino, R.; Iizuka, T.; Ishimura, Y. *J. Biol. Chem.* **1987**, *262*, 4549. (d) Tsubaki, M.; Hiwatashi, A.; Ichekawa, Y. *Biochemistry* **1986**, *25*, 3563.

(10) Evangelista-Kirkup, R.; Smulevich, G.; English, A.; Spiro, T. G. *Biochemistry* **1986**, *25*, 4420.

(11) Smulevich, G.; Evangelista-Kirkup, R.; Spiro, T. G. *Biochemistry* **1986**, *25*, 4426.

(12) Yu, N.-T.; Kerr, E. A.; Ward, B.; Chang, C. K. *Biochemistry* **1983**, *22*, 4534.

(13) Ward, B.; Wang, C. B.; Chang, C. K. *J. Am. Chem. Soc.* **1981**, *103*, 5236.

(14) Parthasarathi, N.; Spiro, T. G. *Inorg. Chem.* **1987**, *26*, 3792.

(15) Benko, B.; Yu, N.-T. *Proc. Natl. Acad. Sci. U.S.A.* **1983**, *80*, 7042.

Table II. Vibrational Frequencies (cm^{-1}) of FeCO Linkage in Carbonyl Complexes of Metalloporphyrins and Heme Proteins

	molecule	ν_{FeCO}	$\Delta^{13}C$	$\Delta^{18}O$	ν_{CO}	$\Delta^{13}C$	$\Delta^{18}O$	δ_{FeCO}	$\Delta^{13}C$	$\Delta^{18}O$	ref
1	HRP low pH	537	4	8	1904	42	42	587	20		10, 9c
2	CCP low pH	530			1922			585			11
3	*Glycera dibranchiata* poly Hb	520	6		1932	44		580	16		41a
4	FeSP-13(*N*-MeIm)	514	4		1932	44		579	12		12
5	elephant Mb	515	3	6	1937	(91)[a]		579	16	1	26
6	FeSP-14(*N*-MeIm)	512	4	5	1939	45		578	15	3	12
7	sperm whale Mb	512	3	8	1944	48	48	577	14	1	33a
8	FeSP-15(*N*-MeIm)	509	6		1945	44		574	11		12
9	leghemoglobin	505			1948			580			41b–d
10	carp Hb	508			1951						33, 41e
11	human Hb A	507	4	9	1951	43	43	578	15	2	33
12	CCP high pH	503			1948			575			11
13	heme-5(*N*-MeIm)	495	4	9	1954	44					12
14	insect Hb CTT III	500			1960			574			36
15	(ImH)Fe^{II} 495 (PP IX DME)	495			1960						10
16	*Glycera dibranchiata* poly Hb	498	3		1963	47					41a
17	Fe(T_{iv}PP) (1,2-Me_2Im)	496	5		1962						41f, g
18	*Glycera dibranchiata* Hb	496	4		1967						41a
19	Fe(T_{iv}PP)(*N*-MeIm)	489	4	8	1966						41f, g
20	carp Hb IHP	491			1968						33, 44e, h
21	Fe^{II}(OEP), (4-NH_2Py)	493			1971						41f, i
22	Fe^{II}TPP(py)	484	4	9	1976	43	43				2a, 26, 41f
23	Fe^{II}(T_{iv}PP) (THF)	526	5	10	1957						41g
24	cyt oxidase	520	4		1964	46		578	14		21a, b
25	CCP	495			1922						11
26	HRP high pH	490	5	10	1932	42	42				10
27	cyt P-450 putidare doxin (from *P. putida*)	483			1932						16a
28	Fe^{II}(PP DME)(Im^-)	492			1942						10
29	cyt P-450 from *P. putida*	481	3	8	1940	43		558	14	3	16a
30	cyt P-450 from bovine adrenocotrical mitochondria	477	7		1953	46					16b
31	Cyt $P\text{-}450_{cam}$ 464 from *P. putida*	464			1963	45		556			16a

[a] Isotopic shift upon $^{13}C^{18}O$ substitution.

angular displacements for the three distortion coordinates. The required energy for a given off-axis displacement of the O atom is found to increase strongly in the order FeCO tilting < porphyrin buckling < FeCO bending. The actual molecular distortion probably involves contributions from all three coordinates with FeCO tilting playing the major role.

Results and Discussion

A. Vibrational Pattern: Electronic Factors. 1. Vibrational Frequencies Reflect Back-Bonding Changes. C–O stretching (ν_{CO}), Fe–C stretching (ν_{FeC}), and Fe–C–O bending (δ_{FeCO}) frequencies are available from infrared and resonance Raman studies of a large number of heme–CO adducts. Table II lists cases where at least two of these frequencies have been determined. These data have been discussed extensively by Kerr and Yu,[8] who examined the strong negative correlation between ν_{FeC} and ν_{CO}. This correlation has been noted by several workers[9] and is shown in Figure 1, which contains extra examples taken from recent work in this laboratory on horseradish peroxidase (HRP)[10] and cytochrome *c* peroxidase (CCP).[11] The negative correlation is attributable to Fe $d_\pi \rightarrow$ CO π^* back-donation; as this increases, the FeC bond order goes up and the CO bond order goes down. Most of the points fall on a single straight line given by

$$\nu_{FeC}\ (cm^{-1}) = 1935 - 0.73\nu_{CO}$$

The −0.73 slope means that the ν_{FeC} frequency shift is 73% of the ν_{CO} frequency shift for a unit change in back-bonding. Since the ν_{CO} frequency is ~4 times the ν_{FeC} frequency and the force constant scales with the square of the frequency, it is evident that the FeC bond is more strongly affected than the CO bond by back-bonding changes. A correlation has also been noted[9c] between δ_{FeCO} and ν_{FeC} but is much weaker, the range of δ_{FeCO} frequencies being small. With the exception of the cytochrome P-450 adducts,[16] δ_{FeCO} is within 5 cm^{-1} of 580 cm^{-1} for all the known heme–CO adducts (Table II).

The points falling significantly off the line reflect changes in the nature of the axial ligand trans to the bound CO. Those below the line belong to strong donor ligands, imidazolate (point 28) and strongly H-bonded imidazole (HRP and CCP, points 25 and 26) or thiolate (the cytochrome P-450 examples (points 27–30)); the increased electron density at Fe enhances back-bonding, as reflected in the lowered ν_{CO}, but the compensating increase in FeC bond order is overridden by competition between the CO and trans donor ligand for the Fe σ orbital (d_{z^2}), leading to a net lowering of ν_{FeC}.[10] Conversely, points falling above the line belong to weak donor ligands, tetrahydrofuran (point 23), and the weakly bound imidazole (as seen in the low iron imidazole stretching frequency in the unligated form[21,22]) of the heme a_3 group in cytochrome oxidase (point 24).

The remaining points fall within 3 cm^{-1} (in ν_{FeC}) of the line and have normal imidazole ligands (except (CO)(Py)FeTPP (Py = pyridine, TPP = tetraphenylporphine) (point 22); evidently pyridine is about the same as imidazole with respect to its σ donor strength). These heme–CO complexes differ only in the extent of their back-bonding. All the CO, imidazole protein-free adducts are in this category including the "strapped" hemes, in which an

(16) (a) Uno, T.; Nishimura, Y.; Makino, R.; Iizuka, T.; Ishimura, Y.; Tsuboi, M. *J. Biol. Chem.* **1985**, *260*, 2023. (b) Makino, R.; Iizuka, T.; Ishikawa, Y. *Proceedings of the IXth International Conference on Raman Spectroscopy*, Tokyo, Japan, Aug 27–Sept 1, 1984; p 492. (c) Tsubaki, M.; Matsusaka, K.; Ichikawa, Y. *Ibid.* p 752.

(17) Teraoka, J.; Kitagawa, T. *Biochem. Biophys. Res. Commun.* **1980**, *93*, 694; *J. Biol. Chem.* **1981**, *256*, 3969.

(18) Stein, P.; Mitchell, M.; Spiro, T. G. *J. Am. Chem. Soc.* **1980**, *102*, 7795.

(19) Poulos, T. L.; Kraut, J. *J. Biol. Chem.* **1980**, *255*, 8199.

(20) Poulos, T. L.; Finzel, B. C.; Gunsalus, I. C.; Wagner, G. C.; Kraut, J. *J. Biol. Chem.* **1985**, *260*, 16122.

(21) (a) Argade, P. V.; Ching, Y. C.; Rousseau, D. L. *Science (Washington, D.C.)* **1984**, *225*, 329. (b) Yoshikawa, S.; Choc, M. G.; O'Toole, T.; Caughey, W. S. *J. Biol. Chem.* **1977**, *252*, 5498.

(22) Ogura, T.; Hon-Nami, K.; Oshima, T.; Yoshikawa, S.; Kitagawa, T. *J. Am. Chem. Soc.* **1983**, *105*, 7781.

(23) Kadish, K. M. In *Iron Porphyrins*; Lever, A. B. P., Gray, H. B., Eds.; Addison-Wesley: Reading, MA, 1982; Part II, pp 161–249.

(24) Evangelista-Kirkup, R.; Crisanti, M.; Poulos, T. L.; Spiro, T. G. *FEBS Lett.* **1985**, *190*, 221.

(25) de Ropp, J. S.; Thanabal, V.; La Mar, G. N. *J. Am. Chem. Soc.* **1985**, *107*, 8268.

Table III. Normal-Mode Frequencies (cm^{-1}) and Isotopic Shifts for Linear L-Fe-C-O[a] (L = *N*-MeIm)

frequencies			$\Delta(^{13}C^{16}O)$		$\Delta(^{12}C^{18}O)$		$\Delta(^{13}C^{18}O)$		$\Delta(^{54}Fe)$	
obsd[b]	calcd	description	obsd	calcd	obsd	calcd	obsd	calcd	obsd	calcd
1954	1954.0	ν_{CO}	44	44.4	44	44.7	90	90.4		0
(578)[c]	583.7	δ_{FeCO}	(15)[c]	17.5	(2)[c]	5.4	(18)[c]	23		−0.6
495	495.5	ν_{FeC}	4	4.2	9	9.4	11	13		−3.8
	244.2	ν_{FeL}		1.3		2.6	~	3.8		−0.9
	164.0	δ_{LFeC}		0		3.1		2.8		−1.6

[a] Force constants K_{CO} = 15.52, K_{FeC} = 2.48, K_{FeL} = 1.6, $k_{FeC,CO}$ = 0.8 mdyn/Å; H_{FeCO} = 0.8, H_{LFeC} = 0.8 mdyn·Å/rad². [b] Data for heme-5-(*N*-MeIm) except δ_{FeCO}. [c] δ_{FeCO} for HbCO.

organic linkage covers the binding region[13] and which were prepared specifically to examine the consequences of steric hindrance to CO binding. Relative to the unhindered adducts, they show higher ν_{FeC} and lower ν_{CO}, i.e. greater back-bonding. Likewise, the heme protein adducts fall on the line (except for those with anomalously strong or weak axial ligands) including myoglobin. *Thus, the vibrational consequences of steric hindrance to CO binding are limited to changes that can be attributed to back-bonding variations.*

But there are other influences that have a larger effect on back-bonding. Point 22, at the low end of the line, belongs to a tetraphenylporphine (TPP) adduct; TPP is less electron-donating than protoporphyrin, and the lower electron density on Fe means less back-donation. Point 1, at the top end of the line, belongs to a HRP conformer having a strong H bond to the bound CO from a titratable protein residue, probably histidine; this H bond is revealed in a 2.5-cm^{-1} downshift of ν_{CO} in D_2O.[7f] The H bond polarizes the CO ligand and enhances back-donation from the Fe. Other polar interactions in the heme pocket may account for much of the variation of the heme protein points along the line.

Myoglobin has a distal histidine, whose disposition, along with that of a valine residue, produces the off-axis binding of the CO.[1a] There is no H-bond interaction,[1b] but it is not impossible that the closely contacted imidazole residue is sufficiently polar to enhance back-bonding. This possibility is reinforced by Kerr et al.'s[26] study of elephant myoglobin, in which the distal histidine is replaced by glutamine. Since glutamine has a smaller side chain than histidine, it was anticipated that elephant Mb would contain a more perpendicular FeCO unit and would therefore show vibrational frequencies closer to the protein-free analogue. On the contrary, elephant Mb (point 5) is slightly higher on the line than sperm whale Mb (point 7).[26] The likeliest explanation of this result is that the glutamine amide side chain forms a stronger polar interaction with the bound CO than does the imidazole.

This interpretation is supported by the recent results of Nagai et al.[27] on hemoglobin mutants involving substitutions of the β-chain distal histidine. When this residue[37] was replaced by glutamine, there was no effect on ν_{FeC} or ν_{CO}. The crystal structure shows that the Glu E7 N^{ϵ} atom can occupy the same position as the His E7 N^{ϵ} and can therefore exert a similar polar effect. When His E7 was replaced by the nonpolar residues valine or glycine, however, ν_{FeC} decreased to 493 cm^{-1} while ν_{CO} increased to ~1970 cm^{-1}, consistent with weakened back-bonding due to the loss of the His E7 polar interaction.

In summary we see that the pattern of ν_{FeC} and ν_{CO} frequencies can be understood on the basis of competition for σ bonding between the bound CO and the trans ligand, superimposed on variations in back-bonding. These variations can be due to electron-withdrawing effects of the porphyrin substituents and to polarization by groups in the distal region of the bound CO. Because heme–CO adducts with imidazole ligands all fall on the same straight line *whether or not* there is steric hindrance to perpendicular binding, it is possible to conclude that the effects of the resulting distortion on the vibrational data is limited to an augmentation of Fe → CO back-bonding. If geometry changes produced some other effect, the ν_{FeC} and ν_{CO} points representing off-axis CO adducts should have deviated from the line.

2. FeCO Bending Mode Enhancement. RR spectra of heme proteins frequently exhibit the FeCO bending mode with variable intensity, but it has not been detected in protein-free porphyrin adducts except in the case of the strapped hemes. Yu et al.[12] proposed that δ_{FeCO} activation is a marker for off-axis binding and suggested an activation mechanism involving overlap of the CO π^* and porphyrin π orbitals via tilting of the FeCO unit toward a pyrrole N atom. The observation of δ_{FeCO} in the strapped heme adducts was taken as confirmation of this proposal.[12] On the other hand, elephant MbCO also showed substantial intensity for δ_{FeCO}[26] despite the expected relief of steric hindrance via the distal histidine/glutamine substitution.

The δ_{FeCO} mode is of *E* symmetry in the ideal C_{4v} point group of a heme–CO adduct with FeCO normal to the heme plane. It is therefore not subject to the dominant Franck–Condon (*A* term) mechanism of RR enhancement. Nor is it subject to vibronic (*B* term) enhancement associated with mixing of the in-plane (*E*) electronic transitions,[28] since the *E* representation is not contained in the cross product $E \times E = A_1 + A_2 + B_1 + B_2$. (Vibronic mixing of in-plane (*E*) and out-of-plane (A_1) transitions would

(26) Kerr, E. A.; Yu, N.-T.; Bartnicki, D. E.; Mizukami, H. *J. Biol. Chem.* **1985**, *260*, 8360.
(27) Nagai, K.; Luisi, B.; Shih, D.; Miyazaki, G.; Imai, K.; Poyart, C.; De Young, A.; Kwiatkowsky, L.; Noble, R. W.; Lin, S.-H.; Yu, N.-T. *Nature (London)* **1987**, *329*, 858.
(28) Spiro, T. G. In *Iron Porphyrins*; Lever, A B. P., Gray, H. B., Eds.; Addison-Wesley: Reading, MA, 1982; Part II, pp 89–160.
(29) (a) Choi, S.; Spiro, T. G. *J. Am. Chem. Soc.* **1983**, *105*, 3683. (b) Spiro, T. G.; Stein, P. *Annu. Rev. Phys. Chem.* **1977**, *28*, 501.
(30) Wright, P. G.; Stein, P.; Burke, J. M.; Spiro, T. G. *J. Am. Chem. Soc.* **1979**, *101*, 3531.
(31) Mitchell, M.; Li, X.-Y.; Kincaid, J. A.; Spiro, T. G. *J. Phys. Chem.* **1987**, *91*, 4690.
(32) Jones, L. H.; McDowell, R. S.; Goldblatt, M.; Swanson, B. I. *J. Chem. Phys.* **1972**, *57*, 2050.
(33) (a) Tsubaki, M.; Srivastava, R. B.; Yu, N.-T. *Biochemistry* **1982**, *21*, 1132. (b) Naik, V. M.; Champion, P. M. *Bull. Am. Phys. Soc.* **1987**, *32*, 479.
(34) (a) Bajdor, K.; Oshio, H.; Nakamoto, K. *J. Am. Chem. Soc.* **1984**, *106*, 7273. (b) Watanabe, T.; Ama, T.; Nakamoto, K. *J. Phys. Chem.* **1984**, *88*, 440.
(35) (a) Jameson, G. B.; Molinaro, F. S.; Ibers, J. A.; Collman, J. P.; Brauman, J. I.; Rose, E.; Suslick, K. S. *J. Am. Chem. Soc.* **1984**, *102*, 3224. (b) Brunner, H. *Naturwissenschaften* **1974**, *61*, 129. (c) Duff, L. L.; Appelman, E. H.; Shriver, D. F.; Klotz, I. M. *Biochem. Biophys. Res. Commun.* **1979**, *90*, 1098.
(36) Yu, N.-T.; Benko, B.; Kerr, E. A.; Gersonde, K. *Proc. Natl. Acad. Sci. U.S.A.* **1984**, *81*, 5106.
(37) Hoffman, R.; Chen, M. M. L.; Thorn, D. L. *Inorg. Chem.* **1977**, *16*, 503.
(38) Choi, S.; Spiro, T. G.; Langry, K. C.; Smith, K. N.; Budd, D. L.; La Mar, G. N. *J. Am. Chem. Soc.* **1982**, *104*, 4345.
(39) (a) Spiro, T. G.; Burke, J. M. *J. Am. Chem. Soc.* **1976**, *98*, 5482. (b) Stong, J. D.; Burke, J. M.; Daly, P.; Wright, P.; Spiro, T. G. *J. Am. Chem. Soc.* **1980**, *102*, 5815.
(40) (a) Case, D. A.; Karplus, M. *J. Mol. Biol.* **1978**, *123*, 697–701. (b) Alben, J. O.; Beece, D.; Bowne, S. F.; Doster, W.; Eisenstein, L.; Frauenfelder, H.; Good, D.; McDonald, J. D.; Marden, M. C.; Moh, P. P.; Reinisch, L.; Reynolds, A. H.; Shyamsunder, E.; Yue, K. T. *Proc. Natl. Acad. Sci. U.S.A.* **1982**, *79*, 3744.
(41) (a) Carson, S. D.; Constantinidis, I.; Satterlee, J. D.; Ondrias, M. R. *J. Biol. Chem.* **1985**, *260*, 8741. (b) Fuchsman, W. H.; Appleby, C. A. *Biochemistry* **1979**, *18*, 1309. (c) Armstrong, R. S.; Irwin, M. J.; Wright, P. *J. Am. Chem. Soc.* **1982**, *104*, 626. (d) Rousseau, D. L.; Ondrias, M. R.; La Mar, G. N.; Kong, S. B.; Smith, K. M. *J. Biol. Chem.* **1983**, *258*, 1740. (e) Onwubiko, H. A.; Hazzard, J. H.; Noble, R. W.; Caughey, W. S. *Biochem. Biophys. Res. Commun.* **1982**, *106*, 223. (f) Kerr, E. A. Ph.D. Dissertation, Georgia Institute of Technology, Atlanta, GA, 1984. (g) Kerr, E. A.; Mackin, H. C.; Yu, N.-T. *Biochemistry* **1983**, *22*, 4373. (h) Rousseau, D. L.; Tan, S. L.; Ondrias, M. R.; Ogawa, S.; Noble, R. W. *Biochemistry* **1984**, *23*, 2857. (i) Alben, J. O.; Caughey, W. S. *Biochemistry* **1968**, *7*, 175.

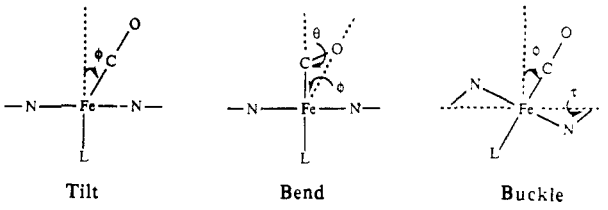

Figure 2. Three possible distortion coordinates for displacing the O atom from the heme normal in CO adducts. For a fixed O atom displacement from the heme normal, the geometrical relations among the tilt (ϕ), bend (Θ), and buckle (τ) angles are $\Theta = 180 - \{\phi + \sin^{-1}[(d_{FeC}/d_{CO})\sin\phi]\}$ and $\tau = \sin^{-1}[(d_{FeN}/d_{NC_\alpha})(\sin\phi/\cos {}^1/_2\eta)]$, where $d_{xy} = x$–y bond distance and $\eta = C\alpha NC\alpha$ of the pyrrole rings. For a 0.9-Å O atom displacement (average value for MbCO[1a]), $\phi = 18°$, $\Theta = 53°$, or $\tau = 48°$ (assuming[2a] $d_{FeC} = 1.77$ Å, $d_{CO} = 1.12$ Å, $d_{FeN} = 2.00$ Å, $d_{NC_\alpha} = 1.38$ Å, and $C_\alpha NC_\alpha = 107°$).

activate an *E* vibration,[29a] but out-of-plane transitions are not generally available.) The lack of δ_{FeCO} intensity in unconstrained heme–CO adducts is therefore not surprising. Activation requires a reduction in molecular symmetry, so that δ_{FeCO} becomes a totally symmetric mode. Off-axis binding would, of course, produce the required symmetry reduction.

It cannot be excluded, however, that electronic influences in the vicinity of the bound CO can also activate δ_{FeCO}, provided they destroy the effective 4-fold symmetry of the heme. If they are themselves directed off axis, the H-bond and polar interactions discussed in the preceding section might be effective in shifting the excited-state heme potential along the FeCO bending coordinate as required for *A*-term RR intensity.[29b] In the π–π^* excited-state electrons are shifted out toward the end of the bound CO, due to the decreased competition from the porphyrin π^* orbitals for back-donation of the Fe d_π electrons. Thus, an off-axis polarization of the π charge cloud is expected to stabilize the tilted structure in the excited state. This mechanism could account for δ_{FeCO} activation in elephant Mb,[26] via the possible interaction with the distal glutamine, and perhaps in other heme proteins as well.

B. Force Constants and Frequencies. We next analyze what effect various distortion coordinates *should* have on the vibrational frequencies. Steric hindrance to perpendicular binding can be accommodated by bending or tilting of the FeCO unit, as discussed in the Introduction. We introduce an additional likely distortion coordinate, porphyrin buckling, in which pyrrole rings on opposite sides of the Fe atom tilt up and down, thereby rotating the entire Fe coordination octahedron. Figure 2 illustrates these three distortion coordinates; the geometric relations among the angles for tilting (ϕ), bending (θ), and buckling (τ) are given in the figure caption. (We note that buckling tilts the FeCO in a specific direction, along one of the Fe–N(pyrrole) bonds, although the actual off-axis distortion is not limited in this way.[1] If buckling is allowed along both N–Fe–N axes simultaneously, however, then a combination of two independent values of τ can produce a tilt in any direction.) The influence of these distortions on the vibrational frequencies can conceptually be divided into kinematic effects and force constant changes, which we now consider in turn.

1. Linear Model. Our starting point for the calculation of the vibrational frequencies and isotope shifts (Table III) is a linear tetraatom L–Fe–C–O, where L is an *N*-MeIm ligand with a single dynamical mass, 82 amu. It is known that heterocyclic ligands behave essentially as rigid rings with respect to metal–ligand stretching modes.[30] The L–Fe stretching force constant was taken as 1.6 mdyn/Å, obtained from the symmetric stretching frequency, 200 cm^{-1}, for the bis(imidazole) complexes of iron(II) and iron(III) protoporphyrin,[31] both of which are low spin, as is the CO–heme adduct. The L–Fe–CO bending force constant, 0.8 mdyn·Å/rad^2, was set equal to the trans CO–Fe–CO bending constant of $Fe(CO)_5$.[32] The Fe–C,C–O stretch–stretch interaction constant, 0.8 mdyn/Å, was also taken from $Fe(CO)_5$. The C–O stretching, Fe–C stretching, and Fe–CO bending force constants, which are 16.47 and 2.64 mdyn/Å and 0.5 mdyn·Å/rad^2, respectively, in $Fe(CO)_5$,[32] were adjusted to 15.52 and 2.48 mdyn/Å and 0.8 mdyn·Å/rad^2, respectively, in order to calculate $\nu_{CO} = 1954$ cm^{-1} and $\nu_{FeC} = 495$ cm^{-1}, in agreement with the values observed for the CO adduct of heme-5 (1-MeImH),[12] and $\delta_{FeCO} = 584$ cm^{-1}, close to the frequencies seen in most of the CO adducts in Table II. The isotope shifts as well as the frequencies (calculated with the aid of Schachtschneider's programs GMAT and VSEC[42]) are seen in Table III to be in excellent agreement with the data. Similar results have earlier been reported by Tsubaki et al.[33] Neither δ_{LFeCO} nor Fe–L has definitely been identified, but assignment of ν_{FeL} to a weak band at 317 cm^{-1} has been proposed[43] for monomeric insect hemoglobin; this value is significantly higher than that calculated here. A somewhat lower frequency, 271 cm^{-1}, has been suggested for ν_{FeL} in MbO_2.[44]

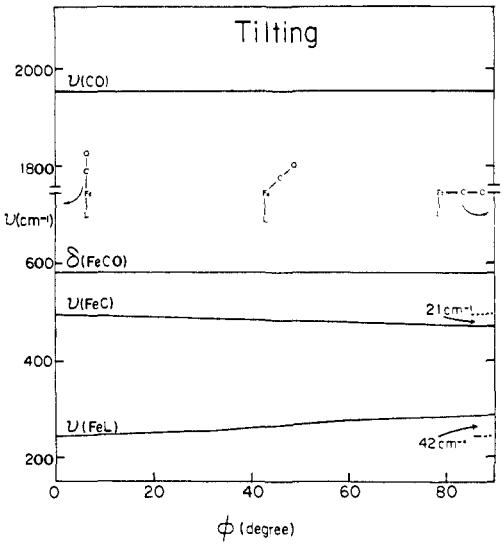

Figure 3. Calculated vibrational frequencies as a function of the tilt angle ϕ, defined in Figure 2. The force constants are the same as in the linear configuration calculation (Table III).

We also investigated whether the FeCO modes might interact with those of the porphyrin macrocycle. Since the L–Fe–C–O bonds are perpendicular to the heme plane, there are no interactions with in-plane modes in the absence of significant off-diagonal force constants. Interactions with porphyrin out-of-plane modes are possible, however, although the insensitivity of ν_{FeCO} to pyrrole ^{15}N substitution[26] suggests that they are not significant. We carried out a calculation with an out-of-plane force field recently developed for nickel octamethylporphyrin[31] and included the L–Fe and Fe–CO bonds in the calculation. Neither the porphyrin modes nor the FeCO modes were perturbed significantly in this calculation; the mixing of these modes is relatively unimportant.

2. Distortion Coordinate Kinematics. Within the context of the linear L–Fe–C–O model, buckling of the porphyrin ring has no kinematic consequences for the vibrational frequencies, since the entire unit is simply rotated relative to the heme plane. There is a small kinematic effect associated with FeCO tilting, provided that the Fe–L bond remains normal to the heme plane, since the interaction between Fe–L and Fe–C stretching coordinates decreases with increasing tilt angle. Figure 3 shows the expected vibrational frequencies as a function of the tilt angle, with the same force constants as in the linear mode calculation (Table III). ν_{FeL} increases appreciably, and ν_{FeC} decreases slightly at large tilt angles; there is no effect on ν_{CO} or δ_{FeCO}.

FeCO bending, on the other hand, introduces a large kinematic effect, because the ν_{FeC} and δ_{FeCO} modes, which are orthogonal as long as the FeCO unit remains linear, mix strongly once it is allowed to bend. Similar conclusions are reported by Naik and

(42) Schachtschneider, J. H. *Vibrational Analysis of Polyatomic Molecules*; Technical Reports 57-65 and 231-64, 1964; Shell Development Co.: Emeryville, CA.
(43) Gersonde, K.; Kerr, E.; Yu, N.-T.; Parish, D. W.; Smith, K. M. *J. Biol. Chem.* **1986**, *261*, 8678.
(44) Walters, M. A.; Spiro, T. G. *Biochemistry* **1982**, *21*, 6989.

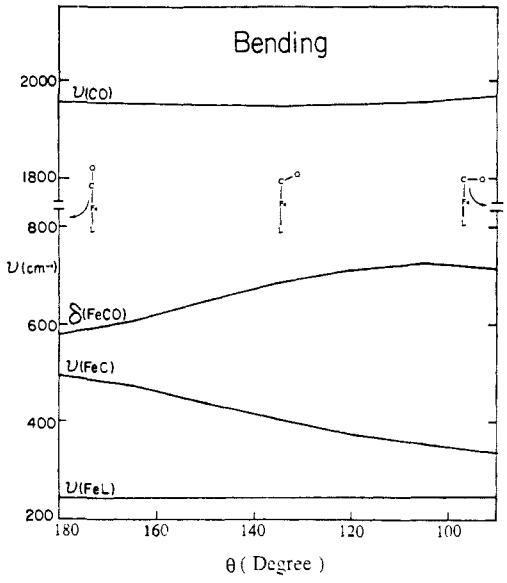

Figure 4. Calculated vibrational frequencies as a function of the FeCO angle θ, defined in Figure 2. The force constants are as given in Table III. δ_{FeCO} and ν_{FeC} become increasingly mixed as θ decreases.

Champion in a preliminary communication.[33b] The two frequencies move rapidly apart with increased bending, as shown in Figure 4, in which the same set of force constants used in the linear model is applied to increasingly bent structures. Not only do the two modes repel one another, but there is a steady change in the normal-mode composition and an interchange between stretching and bending character, as shown in Figure 5, where the potential energy distribution is plotted as a function of the FeCO angle, θ. The upper mode steadily gains FeC stretching character while the lower mode gains bending character as the degree of bending increases. At $\theta < 146°$, the upper mode is primarily FeC stretching in character while the lower mode is primarily FeCO bending. In addition, the contribution of FeL stretching to the lower mode increases at small FeCO angles, as the lower mode frequency approaches ν_{FeL} more closely.

The most characteristic feature of small FeCO angles is the large expected separation, greater than 200 cm^{-1} for θ less than 150°, between the upper and lower bend/stretch modes. Although the mode compositions invert at small angles, the isotope shifts do not do so. Figure 6 shows that the upper mode has the largest ^{13}C shift while the lower mode has the largest ^{18}O shift regardless of the FeCO angle. Thus, the "zigzag" pattern of $^{13}C^{16}O$, $^{12}C^{18}O$, and $^{13}C^{18}O$ shifts, which has been used to identify δ_{FeCO},[8] is *always* characteristic of the upper mode, even when it becomes mainly ν_{FeC} at small FeCO angles. The isotope shift pattern is therefore not a reliable guide to the assignment of stretching or bending character for appreciably bent FeCO. For θ less than 150°, the ^{13}C shift of the upper mode increases noticeably, while the remaining isotope shifts decrease.

The kinematic consequences of bending are nicely illustrated by the study of Nakamoto and co-workers[34] on the O_2 adduct of iron(II) phthalocyanin, for which ν_{FeO} and δ_{FeOO} have been detected in low-temperature RR spectra at 488 and 279 cm^{-1}, respectively. The large difference, 209 cm^{-1}, implies a relatively small FeCO angle. This angle is not known for the phthalocyanin adduct, but it is 129° in a porphyrin analogue, $Fe(O_2)(T_{piv}PP)(2\text{-MeImH})\text{-EtOH}$.[35a] The upper frequency showed a large shift, 21 cm^{-1}, when ^{18}O was substituted for the atom bound to Fe but a very small shift, 1 cm^{-1}, when the outer atom was substituted. Conversely, the lower frequency showed a smaller shift, 2 vs 6 cm^{-1}, when the inner versus the outer atom was substituted. This pattern is fully consistent with the trends shown in Figure 6. Nakamoto and co-workers[34] carried out a triatom normal-coordinate analysis, which successfully reproduced the frequencies and isotope shifts for $\theta = 129°$. They found the upper frequency mode to be FeO stretching primarily. This is what would be expected from Figure 5 at $\theta = 129°$. Nakamoto's work helps to settle a controversy

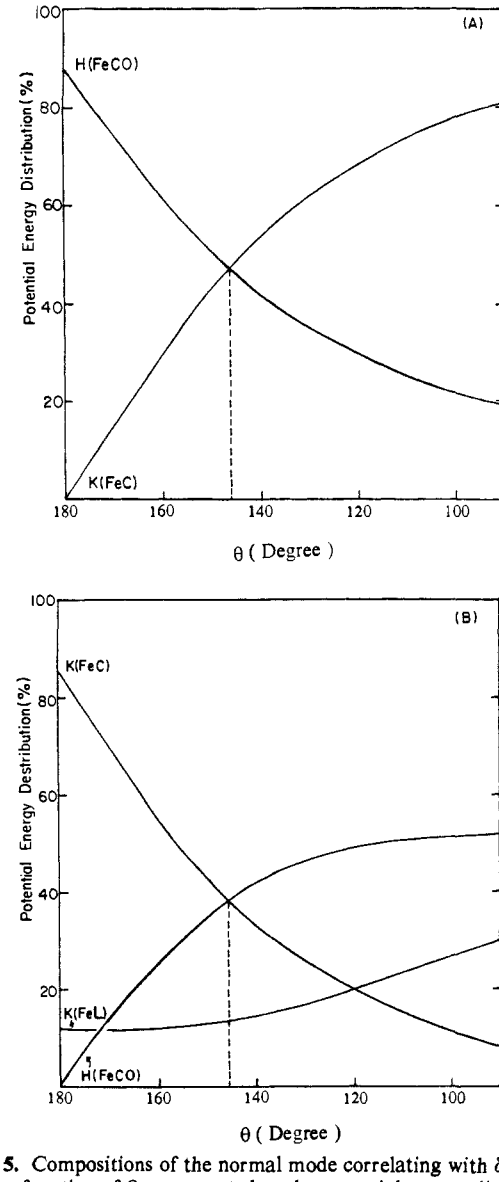

Figure 5. Compositions of the normal mode correlating with δ_{FeCO} and ν_{FeC} as a function of θ, represented as the potential energy distribution among diagonal force constants: (A) upper mode, (B) lower mode.

over the nature of the $^{18}O_2$-sensitive 567-cm^{-1} RR band of HbO_2, first detected by Brunner[35b] and assigned by him to ν_{FeO}. This assignment was questioned by Benko and Yu[15] who called attention to the much smaller isotope shift when the outer vs the inner O atom is substituted with ^{18}O[35c] and suggested reassignment to δ_{FeOO}, based on the analogy with the zigzag isotope shift pattern of δ_{FeCO} in the heme–CO adducts. The present calculations make it clear, however, that the upper frequency always shows this pattern, regardless of the degree of stretching or bending character of the mode. For the relatively small θ expected in O_2–heme adducts, the upper mode must be primarily stretching in character.

Clearly, a wide divergence between ν_{FeC} and δ_{FeCO} modes is not seen in the data on heme–CO adducts (Table I). The range of differences between the two frequencies is 50–80 cm^{-1}. Thus, kinematic considerations alone argue against significant bending in any of the CO adducts. The small values of θ, 120–140°, suggested by the crystallographic[1a] and EXAFS[6] analyses are expected to produce much larger frequency separations, ~250–300 cm^{-1}. This conclusion is not limited by the particular values of the force constants chosen in the calculation. Trial calculations gave a large gap between the two frequencies for a wide range of FeC stretching and FeCO bending constants.

The only way to reduce the δ_{FeCO}/ν_{FeC} divergence is to introduce a large positive FeC,FeCO stretch–bend interaction force constant. Calculations that included this effect showed that a separation

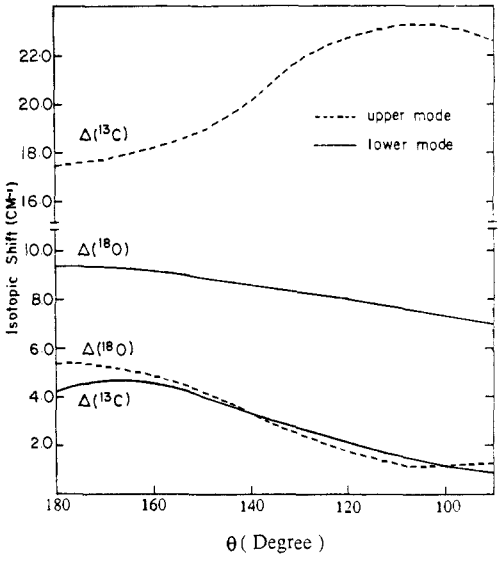

Figure 6. Calculated isotopic shifts for the δ_{FeCO}/ν_{FeC} modes as a function of Θ.

as small as 70 cm^{-1} can be reached in this way with interaction constants of 0.3, 0.4, and 0.7 mdyn/rad when Θ = 165, 150, and 135°, respectively. These values correspond to 20, 30, and 50% of the geometric mean of the stretch and bend valence force constants, 2.5 mdyn/Å and 0.8 mdyn·Å/rad^2. Interaction constants are generally <10% of the geometric mean of the primary force constants being connected. In any event the stretch–bend interaction is expected to be negative, not positive, since bending the FeCO unit decreases π back-bonding (vide infra), thereby weakening the FeC bond and making it easier to stretch. Moreover, it is completely unphysical that the interaction constant should increase strongly with decreasing Θ, as required in order to keep the mode separation in the observed range.

We therefore conclude that FeCO angles anywhere near the 120–140° range required to explain the MbCO X-ray data on the basis of a bent FeCO are not compatible with the vibrational frequencies.

3. Force Constant Changes. Superimposed on kinematic effects are the force constant changes, which may be associated with the various distortion coordinates as a result of electronic factors. The largest bonding change is expected for bent FeCO since the bending coordinate has a strong influence on the nature of the molecular orbitals. This influence has been analyzed by Hoffman and co-workers,[37] whose orbital correlations with bending is shown in Figure 7. The biggest effect is a sharp increase in the energy of the bonding orbital formed by the metal d_π and CO π^* orbitals in the bending plane ($xz + \pi^*$), due to σ–π interaction in the bent structure, which mixes in antibonding character. Consequently, Fe → CO back-bonding is expected to be substantially reduced in bent FeCO. Clearly, this expectation is opposite to the increase in ν_{FeC} observed for MbCO or the strapped heme adducts, relative to the unconstrained models.

For the tilting and buckling coordinates, the FeCO unit remains linear and bonding changes depend on interactions with the porphyrin orbitals. There is competition for the Fe d_π electrons between the CO and porphyrin π^* orbitals. This competition can be seen in the pattern of the porphyrin high-frequency skeletal-mode frequencies, which show an underlying dependence on the porphyrin core size.[38] When the low-spin complex $(ImH)_2Fe^{II}PP$ is examined, there are large deviations from the core-size plots, which can be attributed to back-donation into the porphyrin e_g^* orbitals and the resultant changes in the ring π bonding.[37] If CO replaces one of the ImH ligands, these deviations are reduced,[39] reflecting a shift of the back-bonding electrons from the porphyrin to the CO π orbitals. If the porphyrin were buckled, then the N orbitals of the tilted pyrroles would be misaligned for optimal overlap with the Fe d_π orbital in the buckling plane. There would be a net decrease of Fe → porphyrin back-bonding and therefore a net increase in Fe → CO back-bonding.

Increased back-bonding is also the expected effect of FeCO tilting, which would similarly misalign the Fe and porphyrin π orbitals, provided that CO plays the dominant role in orienting the Fe π orbital. This seems likely since the porphyrin skeletal-mode frequencies show bound CO to relieve the greater part of the frequency shifts associated with Fe → porphyrin back-bonding.[39] Thus, the electronic effects of buckling and tilting are in a direction consistent with the vibrational data.

C. Distortion Coordinate Energetics and the Nature of Off-Axis Binding. We now address the question of what distortion is expected on energetic grounds if there is steric hindrance to perpendicular binding. The heme–CO geometry should adjust to such hindrance via the distortion coordinates offering the least resistance. There are two factors in the energy associated with a particular distortion, the displacement along the coordinate, q, and the shape of the potential well. Within the harmonic approximation, $E = 1/2kq^2$, where k is the force constant. We consider the energy required to move the O atom of the bound CO 0.9 Å away from the heme normal. This is the average displacement reported for the two partially occupied sites of the bound CO in MbCO.[1a] If this displacement were accommodated by FeCO bending, FeCO tilting, or porphyrin buckling, exclusively, the required angular displacements would be $180 - \Theta = 47°$, $\phi = 18°$, or $\tau = 48°$. The bending force constant is $H_{FeCO} = 0.8$ mdyn·Å/rad^2, taken from the linear model calculation, above. For FeCO tilting, the required force constant is that associated with the C–Fe–N(pyrrole) angle; in the absence of an assigned frequency for this vibrational mode, we use the axial–equatorial C–Fe–C bending constant[32] of $Fe(CO)_5$, 0.72 mdyn·Å/rad^2. The porphyrin buckling coordinate involves the simultaneous tilting of two pyrrole rings, each of which swivels about two C_α–C_m bonds. We therefore take the C_α–C_m torsion force constant, estimated in a recent analysis of the porphyrin out-of-plane force field,[31] to be 0.13 mdyn·Å/rad^2 and multiply it by 4 to obtain $k_\tau = 0.52$ mdyn·Å/rad^2.

Assuming that these force constant estimates are reasonable, the harmonic approximation then gives 39, 5, and 27 kcal/mol for the energy required to move the O atom 0.9 Å from the heme normal via bending, tilting, or buckling, respectively. (Case and Karplus estimated 20 kcal/mol for 45° FeCO bending, using a smaller force constant transferred from $Cr(CO)_6$, and 7 kcal/mol for 23° tilting.[40a]) These energies should be taken as upper limits to the actual energies since deviations from the harmonic approximation are no doubt significant for the large angular displacements involved, and anharmonic terms, which reflect electronic relaxation, will reduce the energies. Nevertheless, it is clear that FeCO tilting is much the lowest energy coordinate, while porphyrin buckling is somewhat lower in energy than FeCO bending. We had initially expected that porphyrin buckling would be a low-energy pathway since pyrrole tilting is a facile motion. The angular displacement required for a significant O atom displacement is large, however, since the lever arm for the buckling distortion, the perpendicular distance from a pyrrole N atom to the line connecting the two C_α atoms, is quite short, 0.85 Å.

The actual molecular potential for O atom displacement from the heme normal is expected to be some combination of these three, and perhaps other, distortion coordinates. We assume equipartition of energy among the bending, tilting, and buckling coordinates and calculate that a 0.9-Å O atom displacement would require $180 - \Theta = 9°$, $\phi = 9.5°$, and $\tau = 11°$ for a total energy of 4.2 kcal/mol, in the harmonic approximation. Thus, the individual angular displacements are markedly reduced if all three distortion coordinates contribute. They become sufficiently small so that the harmonic approximation should be reasonable. The total energy is slightly less than that required for tilting alone and is small enough that the protein could reasonably be expected to support the force required for the distortion, as discussed by Case and Karplus.[40a]

With respect to the vibrational frequencies, the expected effects of the three distortion coordinates would add to one another. Since back-bonding is predicted to be decreased by bending but increased

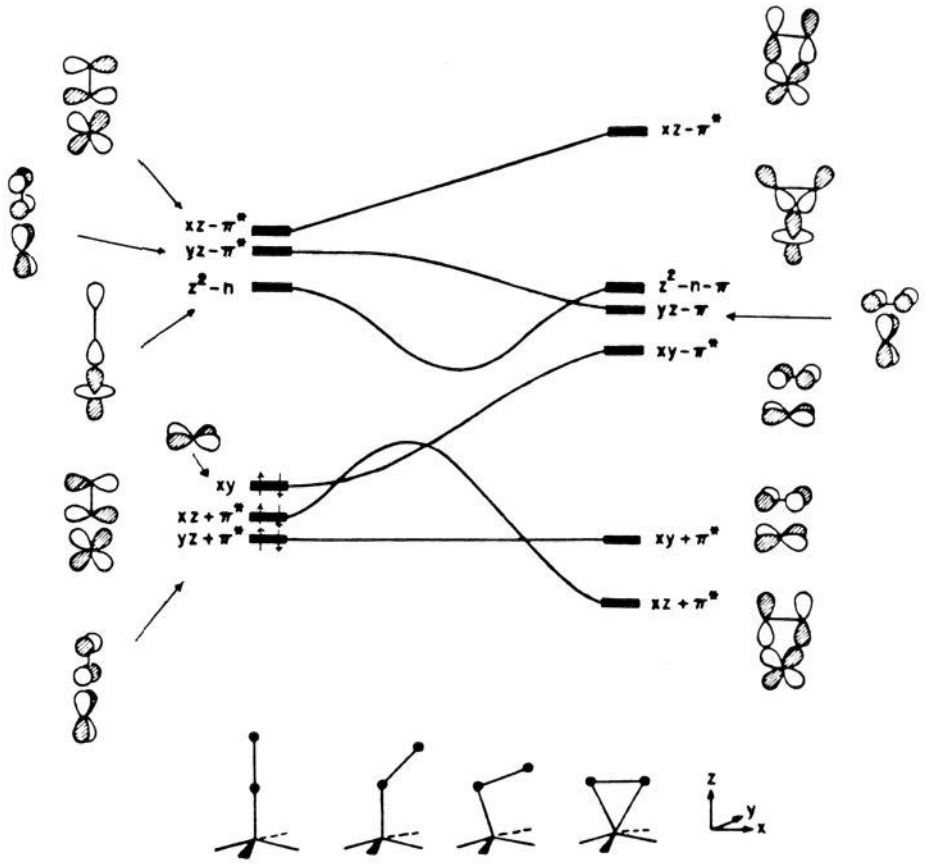

Figure 7. Orbital correlation diagram for bending of a L_4MXY fragment, adapted from ref 37. The electron occupancy is shown for $Fe^{II}CO$. Bending strongly destabilizes the d_{xz} + CO π^* bonding orbital and decreased back-donation.

by tilting and buckling, the net change may be smaller than might otherwise have been expected for the large deviation from perpendicular binding observed for MbCO. The kinematic effects of bending are expected to push δ_{FeCO} and ν_{FeC} apart, but at 180° − Θ = 9° the magnitude of the separation increases relative to the linear model; 17 cm^{-1} (see Figure 4) could only be detected with accurately calibrated distortion models.

The question arises as to how consistent this view of a concerted distortion is with the available structure data. The X-ray crystal structure data for MbCO at 1.5-Å resolution shows clear evidence for disordered CO.[1a] The final refinement produced two bent FeCO units, with occupancies of 22 and 78%, at Θ = 120 and 141°. Tilted structures were considered, and found to be less satisfactory, but could not be ruled out with confidence. A combination of bending and tilting would therefore not be inconsistent with the data at the present resolution. Porphyrin buckling was not considered explicitly, although all the porphyrin atoms were refined independently. A large degree of pyrrole tilting, as would be required if buckling were the sole distortion coordinate, is not evident in the refined structure, but the small amount of buckling predicted in the concerted distortion model may be possible.

On the other hand, the EXAFS data on MbCO at 4 K has been interpreted as showing a small FeCO angle, Θ = 127 ± 4°. This angle is determined directly from the reduction in second-shell scattering amplitude, which is anomalously high for linear FeCO due to self-focusing. This amplitude was found to be substantially lower for MbCO than for a protein-free linear analogue complex.[6] Tilting and buckling would not change the self-focusing effect, since the FeCO unit remains linear in these distortion coordinates. On the other hand, large contributions to the second-shell scattering are expected from atoms of the porphyrin ring and the imidazole ligand, and it cannot be ruled out that these contributions, and their interferences, are different for MbCO and the linear analogue. Particularly in the case of porphyrin buckling, alteration in the second shell from the porphyrin might well be expected. Thus, alternate explanations of the second-shell amplitude reduction may be possible.

It should be pointed out that the EXAFS data were collected at 4 K, to minimize the Debye–Waller factor and radiation damage, while the RR data are limited from liquid solution because frozen samples are photodissociated by the laser beam. On the other hand, the IR spectrum shows ν_{CO} to be not significantly different at 4 K and room temperature[40] so that a significant structural alteration on freezing to 4 K is unlikely.

Summary

The available vibrational data on heme–CO complexes can be interpreted on the basis of Fe → CO back-donation and its variations. A plot of ν_{FeC} vs ν_{CO} shows a single inverse relationship when imidazole is the axial ligand, whether the complex is in a protein or not, and even when it contains a molecular strap designed to restrain perpendicular FeCO binding. Thus, the effects of geometric distortions in these molecules are limited to changes in the extent of back-bonding. The points for MbCO and the strapped hemes lie somewhat higher on the line than that of an unconstrained heme–CO adduct, indicating that back-bonding is increased slightly by the off-axis binding. This is the direction expected for buckling and tilting distortions but is opposite to that expected for FeCO bending. In any given protein or model the effects of geometric distortions on back-bonding may be compounded with those due to electronic interactions. H bonding from distal groups to the bound CO greatly increases back-bonding, and other polar interactions may also have a significant influence.

While X-ray crystallography and EXAFS results have been interpreted to indicate that MbCO has a strongly bent FeCO unit with Θ ≃ 130°, a normal-coordinate analysis shows the vibrational frequencies to be inconsistent with a significantly bent structure. (A previously proposed equation to calculate the FeCO angle directly from isotope shifts has, however, been shown to be in-

correct; see Appendix.) FeCO bending drives the δ_{FeCO} and ν_{FeC} frequencies strongly apart, as is observed for the O_2 adduct of iron(II) phthalocyanin, due to mixing of the internal coordinates. While the frequencies can be brought back together with a positive FeC,FeCO stretch–bend interaction constant, the sign and magnitude of the constant are unreasonably large, as the required variation with the FeCO angle. The FeCO tilting and porphyrin buckling distortion coordinates have negligible kinematic consequences.

The energy required to produce a given displacement of the O atom from the heme normal increases strongly in the order tilting < buckling < bending, mainly due to the much smaller angular displacement required for tilting. All three coordinates are expected to contribute to the actual molecular distortion on the basis of energy equipartition. In this model the three distortion angles are similar, and small, ~10°. Because the predicted effect on ν_{FeC} is opposite for bending and for tilting or buckling, the net influence on the vibrational pattern may be small. The concerted distortion model, with small angular displacements, is not inconsistent with the MbCO X-ray crystal data at the present resolution and level of FeCO disorder. It is inconsistent with the EXAFS analysis of MbCO at 4 K, from which the FeCO angle is calculated directly via the attenuation of the second-shell scattering relative to a protein-free model. Possibly other second-shell alterations, especially porphyrin buckling, could account for the attenuation.

Acknowledgment. We are grateful to Drs. Martin Karplus, John Kuriyan, and Paul Champion for stimulating and helpful discussions concerning the ideas in this manuscript. This work was supported by NIH Grant GM33576.

Note Added in Proof. Moore et al.[48] have recently used picosecond time-resolved infrared spectroscopy to estimate the angle, α, between the C–O bond and the normal to the heme plane. α was found to be 18° for HbCO and 20° and 35° for the major (ν_{CO} = 1944 cm^{-1}) and minor (ν_{CO} = 1933 cm^{-1}) forms of MbCO. Assuming α to be the sum of the bend ($180 - \theta$) and tilt (ϕ) angles and using the O atom positions of the two X-ray determined conformers,[1a] as well as standard Fe–C and C–O bond distances, Moore et al. calculated θ and ϕ values of 174° and 14° for the ν_{CO} = 1944 cm^{-1} form and 157° and 12° for the ν_{CO} = 1933 cm^{-1} form. Our concerted distortion model is compatible with these estimates since allowing for porphyrin buckling would reduce the required bend and tilt angles somewhat. We thank Dr. Robin Hochstrasser for communicating this information.

Appendix

Isotopic Frequencies and the FeCO Angle. Adapting a kinematic analysis by Champion et al.[45] of the axial ligand mode frequencies in heme–thiolate complexes, Yu et al.[12] proposed the eq 1 to determine the FeCO angle, Θ, where ν_1 and ν_2 are the Fe–C and

$$\sin^2\Theta = \frac{1/M_i^2 - B/M^2}{B/m_2^2 - 1/m_{2i}^2} \qquad B = \left[\frac{\nu_{1i}\nu_{2i}}{\nu_1\nu_2}\right]^2 \tag{1}$$

C–O stretching frequencies, respectively, and $M^2 = m_1m_2m_3/(m_1 + m_2 + m_3)$; m_1, m_2, and m_3 are the Fe, C, and O masses, respectively. The subscript i indicates that the mass or frequency is for a given isotopic substitution.

This equation derives from the general solution to the secular equation for a triatomic oscillator $M_1 - M_2 - M_3$, with bond distances $M_1 - M_2 = d_1$ and $M_2 - M_3 = d_2$, on the assumption that there are no off-diagonal terms (interaction force constants) in the potential energy matrix[46] (eq 2).

$$\lambda^3 + A\lambda^2 + B\lambda + C = 0 \qquad \lambda = 4\pi^2(C\nu)^2 \tag{2}$$

$$A = -\{F_{11}(\mu_1 + \mu_2) + F_{22}(\mu_2 + \mu_3) + F_{33}[d_2^2\mu_1 + d_1^2\mu_3 + (S^2d_+^2 + C^2d_-^2)\mu_2]\}$$

$$B = F_{11}F_{22}[\mu_1\mu_3 + \mu_1\mu_2 + \mu_2\mu_3 + 4C^2S^2\mu_2^2] + F_{11}F_{33}[d_2^2\mu_1^2 + d_1^2\mu_1\mu_3 + (S^2d_+^2 + C^2d_-^2 + d_2^2)\mu_1\mu_2 + d_1^2\mu_2\mu_3 + (S^2d_+^2 + C^2d_-^2 - 4C^2S^2d_1^2)\mu_2^2] + F_{22}F_{33}[d_2^2\mu_1\mu_3 + d_2^2\mu_1\mu_2 + d_1^2\mu_3^2 + (S^2d_+^2 + C^2d_-^2 + d_1^2)\mu_2\mu_3 + (S^2d_+^2 + C^2d_-^2 - 4C^2S^2d_2^2)\mu_2^2]$$

$$C = -\{F_{11}F_{22}F_{33}[d_2^2\mu_1^2\mu_3 + d_2^2\mu_1^2\mu_2 + d_1^2\mu_1\mu_3^2 + (S^2d_+^2 + C^2d_-^2)\mu_1\mu_2^2 + d_1^2\mu_3^2\mu_2 + (S^2d_+^2 + C^2d_-^2)\mu_3\mu_2^2 + (S^2d_+^2 + C^2d_-^2 + d_1^2 + d_2^2)\mu_1\mu_2\mu_3]\}$$

$$C = \cos\left(\frac{\theta}{2}\right) \qquad S = \sin\left(\frac{\theta}{2}\right)$$

$$d_+ = d_2 + d_1 \qquad d_- = d_2 - d_1$$

$$\mu_i = 1/m_i$$

F_{11}, F_{22}, and F_{33} are force constants for stretching d_1 and d_2 and bending Θ, respectively. Champion et al.[45] and Yu et al.[12] simplified eq 2 by dropping all terms in F_{33} on the grounds that $F_{33} \ll F_{11}, F_{22}$; bending force constants are generally much smaller than stretching force constants. For the Fe–S–C linkage of heme–thiolate complexes,[45] this approximation may not be too bad, since the Fe–S–C bending force constant is expected to be quite small. In the case of FeCO, however, the disparity is less than usual since $F_{33} = H_{FeCO}$ = 0.8 mdyn·Å/rad² or ~0.4 mdyn/Å, and $F_{22} = k_{FeC}$ = 2.50 mdyn/Å. It can easily be shown that the magnitudes of the dropped terms are far from negligible. In fact, the terms in F_{33} actually are comparable with the terms in F_{22}. Thus, within the A coefficient (eq 2), the ratio of these terms is

$$\frac{F_{33}[d_2^2\mu_1 + d_1^2\mu_3 + (S^2d_+^2 + C^2d_-^2)\mu_2]}{F_{22}(\mu_2 + \mu_3)} = (F_{33}/F_{22})9 \approx 0.73$$

while, within B coefficient, the ratio is

$$\frac{F_{11}F_{33}[...] + F_{22}F_{33}[...]}{F_{11}F_{22}[\mu_1\mu_2 + \mu_1\mu_3 + \mu_2\mu_3 + 4C^2S^2\mu_2^2]} = (0.406 + 0.05)/0.305 \approx 1.48$$

Consequently neglect of the F_{33} terms cannot lead to a correct equation.

It is possible to simplify eq 2 without dropping any term by introducing the relationship[47]

$$\lambda_1\lambda_2\lambda_3 = F_{11}F_{22}F_{33}/M^2\mu$$

$$\frac{1}{\mu} = \frac{d_2}{d_1}\left(\frac{1}{m_1} + \frac{1}{m_2}\right) - \frac{2}{m_2}\cos\Theta + \frac{d_1}{d_2}\left(\frac{1}{m_2} + \frac{1}{m_3}\right)$$

The remaining quantities are defined above.

For a given isotopic substitution we have eq 3. Rearrangement

$$\frac{\lambda_1'\lambda_2'\lambda_3'}{\lambda_1\lambda_2\lambda_3} = \frac{M^2}{M_i^2}\frac{\mu}{\mu_i}$$

$$\left[\frac{\nu_1'\nu_2'\nu_3'}{\nu_1\nu_2\nu_3}\right]^2 = \frac{M^2}{M_i^2}\frac{\mu}{\mu_i}... \tag{3}$$

of (3) gives eq 4. Equation 4 is a corrected version of eq 2, with all terms retained. The isotopic frequency product ratio, R_ν, now

(45) Champion, P. M.; Stallard, B. R.; Wagner, G. C.; Gersonde, I. C. *J. Am. Chem. Soc.* **1982**, *104*, 5469.

(46) Wilson, E. B., Jr. *J. Chem. Phys.* **1939**, *7*, 1047.

(47) (a) Lechner, F. *Monatsh. Chem.* **1932**, *61*, 385. (b) Kohlrausch, K. W. F. *Der Smekal-Raman Effekt*, Ergänzungsband, 1931–1937; Springer: Berlin, 1938; p 65.

(48) Moore, J. N.; Hansen, P. A.; Hochstrasser, R. M. *Proc. Natl. Acad. Sci. U.S.A.*, in press.

includes the bending mode frequency.

$$\cos\Theta = \frac{m_2 m_2'}{2}\,\frac{\dfrac{d_2}{d_1}\left(\dfrac{1}{\mu_1'} - \dfrac{R_\nu R_m}{\mu_1}\right) + \dfrac{d_1}{d_2}\left(\dfrac{1}{\mu_2'} - \dfrac{R_\nu R_m}{\mu_2}\right)}{m_2 - m_2' R_\nu R_m} \quad \cdots \quad (4)$$

$$R_\nu = \left[\frac{\nu_1'\nu_2'\nu_3'}{\nu_1\nu_2\nu_3}\right]^2 \qquad R_m = (M'/M)^2$$

$$\frac{1}{\mu_1} = \frac{1}{m_1} + \frac{1}{m_2} \qquad \frac{1}{\mu_2} = \frac{1}{m_2} + \frac{1}{m_3}$$

Unfortunately, eq 4 is essentially useless for calculating Θ because R_ν depends very weakly on Θ. Thus, ^{13}C substitution gives calculated values of $R_\nu = 0.879$, 0.881, and 0.889 for $\Theta = 180$, 135, and 90°, while ^{18}O substitution gives $R_\nu = 0.888$, 0.887, and 0.876. The entire range of variation is only 1.1%. On the other hand, a measurement error of only 2 cm^{-1} in either ν_{FeC} or in δ_{FeCO}, well within the usual uncertainty since their RR bands are frequently weak and overlapped with porphyrin bands, produces a ~0.8% error in R. Moreover, the equation remains only approximate since all interaction force constants are neglected; it is known from the $Fe(CO)_5$ vibrational analysis that the FeC,CO stretch–stretch interaction constant is not negligible.[33] When the available ^{13}C isotopic data are examined (Table II), the experimental values of R_ν mostly fall in the range of 0.891–0.902, significantly above the highest calculated value, $R_\nu = 0.889$ for $\Theta = 90°$. Probably this systematic upward shift is associated with the FeC,CO interaction constant. The required correction for this effect adds to the utility of the isotopic shifts in determining the FeCO angle directly.

We conclude that it is not possible to calculate the FeCO angle directly from the vibrational frequencies and isotope shifts. These have to be modeled with a specific force field.

The Reaction of *n*-Butyllithium with Diphenylacetylene: Structure Elucidation of the Mono- and Dilithio Product by One- and Two-Dimensional NMR Spectroscopy, X-ray Analysis, and MNDO Calculations. Agostic Activation by Lithium†

Walter Bauer,‡ Martin Feigel,‡ Gerhard Müller,§ and Paul von Ragué Schleyer*,‡

Contribution from the Institute of Organic Chemistry of the Friedrich-Alexander-Universität Erlangen-Nürnberg, Henkestrasse 42, D-8520 Erlangen, Federal Republic of Germany, and the Institute of Inorganic Chemistry of the Technische Universität München, Lichtenbergstr. 4, D-8046 Garching, Federal Republic of Germany. *Received November 13, 1987*

Abstract: One equivalent of *n*-butyllithium (*n*BuLi) adds to diphenylacetylene (tolane) in tetrahydrofuran (THF) to give the trans product **2** exclusively; this monolithio compound is monomeric in THF. When carried out in hexane/TMEDA solution (TMEDA = *N,N,N',N'*-tetramethylethylenediamine), this reaction is accompanied by the formation of the dilithio product **3**. Both **2** and **3** are characterized by two-dimensional NMR spectroscopy (COSY, C–H shift correlation, COLOC). The known site of the second metalation (H8 in **2**) is "predicted" both by ^1H–^6Li–2D heteronuclear Overhauser spectroscopy (HOESY) and by MNDO calculations, both of which indicate a short Li···H8 distance in **2** ("agostic" interaction). The dimetalation product **3** can be obtained directly in hexane/TMEDA with 2 equiv of *n*BuLi. In the crystalline state, **3** is a doubly lithium bridged monomer chelated with one TMEDA ligand per lithium atom (X-ray). The doubly lithium bridged structure is retained in benzene-d_6 solution. In THF-d_8, however, a temperature and concentration dependent monomer–dimer equilibrium is observed ($\Delta H° = 9.4$ kcal/mol, $\Delta S° = 22.2$ eu). In the dimer **24**, comprised of a central C_4Li_4 cubic moiety, two pairs of nonisochronous lithium atoms give rise to two signals in the ^6Li NMR spectrum; these are assigned by ^1H–^6Li–2D HOESY. Line shape analysis of the temperature dependent ^6Li spectra gives the activation parameters, $\Delta H^‡ = 9.4$ kcal/mol and $\Delta S^‡ = -23.5$ eu, for the dimer–monomer reaction, whereas the exchange of the chemically nonequivalent lithium sites in the dimer proceeds with $\Delta H^‡ = 16.1$ kcal/mol and $\Delta S^‡ = 1.2$ eu. The lithium exchange within the dimer and in the monomer–dimer equilibrium is proven by 2D–^6Li exchange spectroscopy (NOESY). Small scalar couplings between the chemically nonequivalent ^6Li atoms in the dimer **24** are detected by ^6Li–^6Li COSY.

Organolithium compounds are known to add stereo- and regiospecifically to carbon–carbon double and triple bonds.[1] Such reactions have long been used to initiate polymerization[1] and for the synthesis of many otherwise unavailable functionalized alkanes and alkenes.[1-3] The reaction between *n*-butyllithium (*n*BuLi) and diphenylacetylene (**1**) (tolane), studied extensively 2 decades ago by Mulvaney et al.[4-7] was found not only to give **2** but also to proceed beyond the addition stage. Deuteriation and carbonation experiments gave evidence for the formation of a dilithio compound **3** (Scheme I) as well.

The reaction in hexane was accelerated appreciably by the presence of *N,N,N',N'*-tetramethylethylenediamine, TMEDA.[7] An elegant chemical study[6] demonstrated that the mechanism

† Dedicated to Professor Dr. Valentin Freise, University of Regensburg, Federal Republic of Germany, on the occasion of his 70th birthday.

‡ University of Erlangen-Nürnberg.

§ Technical University of Munich.

(1) Wakefield, B. J. *The Chemistry of Organolithium Compounds*; Pergamon: 1974; p 89f.
(2) Wakefield, B. J. In Wilkinson, G., Stone, F. G. A., Abel, E. W., Eds.; *Comprehensive Organometallic Chemistry*; Pergamon: Oxford, 1982; Vol 7, p 1f.
(3) Normant, J. F.; Alexakis, A. *Synthesis* **1981**, 841.
(4) Mulvaney, J. E.; Garlund, Z. G.; Garlund, S. L. *J. Am. Chem. Soc.* **1963**, *85*, 3897.
(5) Mulvaney, J. E.; Garlund, Z. G.; Garlund, S. L.; Newton, D. J. *J. Am. Chem. Soc.* **1966**, *88*, 476.
(6) Mulvaney, J. E.; Carr, L. J. *J. Org. Chem.* **1968**, *33*, 3286.
(7) Mulvaney, J. E.; Newton, D. J. *J. Org. Chem.* **1969**, *34*, 1936.

0002-7863/88/1510-6033$01.50/0